General Disclaimer

One or more of the Following Statements may affect this Document

- This document has been reproduced from the best copy furnished by the organizational source. It is being released in the interest of making available as much information as possible.

- This document may contain data, which exceeds the sheet parameters. It was furnished in this condition by the organizational source and is the best copy available.

- This document may contain tone-on-tone or color graphs, charts and/or pictures, which have been reproduced in black and white.

- This document is paginated as submitted by the original source.

- Portions of this document are not fully legible due to the historical nature of some of the material. However, it is the best reproduction available from the original submission.

NASA TECHNICAL MEMORANDUM

NASA TM-78,434

NASA TM-78,434

EFFECTS OF UNSTEADY AERODYNAMICS ON ROTOR AEROELASTIC STABILITY

Donald L. Kunz

Ames Research Center, NASA
and
Ames Directorate, USAAMRDL, AVRADCOM
Ames Research Center, Moffett Field, Calif. 94035

September 1977

EFFECTS OF UNSTEADY AERODYNAMICS ON ROTOR AEROELASTIC STABILITY

Donald L. Kunz

Research Scientist
Ames Research Center
Ames Directorate

U. S. Army Air Mobility R&D Laboratory
AVRADCOM
Moffett Field, California

Abstract

An analysis was conducted to study the effects of unsteady aerodynamics on the stability characteristics of helicopter rotor blades. A simple physical model of each blade was used together with Theodorsen, Loewy, and quasi-steady aerodynamics to derive the equations of motion. The stability analysis comparing the effects of using each of the three theories revealed some significant differences between the Loewy and Theodorsen results. These included increases and decreases in lead-lag damping, localized around integer lead-lag frequencies. It was also shown that the standard method of multi-blade coordinates must be modified for use in conjunction with Loewy aerodynamics.

Notation

a	Linear, two-dimensional lift curve slope
B	Tip loss factor
$C(k)$	Theodorsen's lift deficiency function
$C(k,m,h,N,\psi_q)$	Loewy's lift deficiency function
C_{d_o}	Profile drag coefficient
c	Blade chord
$\bar{c}$	Nondimensional blade chord, c/R
D	Airfoil section drag force
e	Hinge offset nondimensionalized by R, Fig. 1
h	Wake spacing nondimensionalized by R, Fig. 2
I	Blade inertia about the hinge
$\bar{I}_\theta$	Blade torsional inertia nondimensionalized by I
i	$\sqrt{-1}$
K_2, K_3, K_4	Blade geometry correction factors, Eq. (16)
K_β, K_ζ	Combined flap and lead-lag spring stiffness at $\theta_b = \theta_h = 0$, Eqs. (A10-A11)
$K_{\beta b}, K_{\zeta b}$	Flap and lead-lag spring stiffnesses at the blade root, Fig. 1
$K_{\beta h}, K_{\zeta h}$	Flap and lead-lag spring stiffness of the inclinable hub springs, Fig. 1
k	Reduced frequency, $\omega\bar{c}/2\Omega r$
L_c	Airfoil section circulatory lift force
L_{nc}	Airfoil section noncirculatory lift force
M_{β_a}, M_{ζ_a}	Nondimensional aerodynamic hinge moments
M_{β_e}, M_{ζ_e}	Nondimensional elastic hinge moments
M_{β_i}, M_{ζ_i}	Nondimensional inertial hinge moments

m	Modal frequency ratio, ω/Ω
N	Number of blades
p	Uncoupled rotating flap frequency
Q	Generalized lift deficiency function
Q_1, Q_2, Q_3	Integrated lift deficiency functions, Eq. (17)
q	Blade number (0, 1, 2, . . .)
R	Rotor radius
R_b, R_h	Elastic coupling parameters, Eqs. (A8-A9)
r	Distance outboard of the hub centerline nondimensionalized by R
s	Modal eigenvalue, $\sigma + i\omega$
V	Blade velocity in the plane of rotation, Eq. (12)
x	Distance outboard of the hinge nondimensionalized by R
x_o	Blade root cutout (from the hinge) nondimensionalized by R
$\dot{z}$	Blade velocity normal to the plane of rotation, Eq. (11)
β	Blade flapping deflection, Fig. 1
γ	Lock number, $\rho acR^4/I$
Δ	Stiffness parameter, Eq. (7)
ε	Blade pitch angle with respect to V
ζ	Blade lead-lag deflection, Fig. 1
θ	Blade geometric pitch angle, Fig. 1
θ_b, θ_h	Inclinations of the blade and hub principal flexural axes, Fig. 1
$\theta_\beta, \theta_{\beta_b}, \theta_{\beta_h}$	Pitch-flap coupling parameters, Eqs. (20-22)
$\theta_\zeta, \theta_{\zeta_b}, \theta_{\zeta_h}$	Pitch-lag coupling parameters, Eqs. (20-22)
ρ	Air density
σ	Modal damping

σ_ζ	Lead-lag damping
ϕ_i	Inflow angle
ψ_q	Interblade phase angle
Ω	Rotor rotational speed
ω	Modal frequency
ω_ζ	Lead-lag frequency
$\bar{\omega}_\beta, \bar{\omega}_\zeta, \bar{\omega}_\theta$	Nondimensional, uncoupled flap, lead-lag, and torsion natural frequencies, Eqs. (A12-A13)
$(\ )_o, \Delta(\ )$	Equilibrium and perturbation quantities
$(\dot{\ })$	$[d(\ )/dt]/\Omega$
$(\ddot{\ })$	$[d^2(\ )/dt^2]/\Omega^2$

Introduction

Over the past few years, many investigators have studied the aeroelastic stability of hingeless helicopter rotor blades. For the most part, these researchers have used quasi-steady, strip theory aerodynamics to develop the aerodynamic forces [1-3]. Although the results obtained from such analyses have often correlated well with experiment [4], and have provided valuable insights into the physical problem, some discrepancies have appeared which cannot be explained within the limits of the theory [5]. A possible source of these discrepancies is unsteady aerodynamics.

The aerodynamic theories used in this investigation include Theodorsen's unsteady theory [6], Loewy's rotary-wing theory [7], and a quasi-steady approximation to the two unsteady theories. By comparing the results obtained by using each of these aerodynamic formulations, the relative effects of unsteady flow and the shed wakes beneath the rotor plane can be determined.

While other investigators have used unsteady aerodynamics in stability analyses [8-10], their main concern has generally been the determination of stability boundaries. The primary reason for the limited scope of these analyses has been that the aerodynamic theories only apply for simple harmonic motion. It is the intention of this study to treat transient motion, by assuming that motion to be nearly simple harmonic, as well as the case of neutral stability. In addition, the work presented here observes the effects of the shed wakes below the rotor plane on the behavior of a multibladed rotor.

Blade Model

The physical model chosen to represent each individual blade of the rotor was purposely kept simple, so that the aerodynamic effects would be obscured as little as possible by the blade dynamics. It is the same as the model used for the theoretical development in Reference 5.

As shown in Figure 1, the blade model has flap and lead-lag degrees of freedom, perpendicular and parallel to the plane of rotation. While the blade is rigid in torsion, provisions are made for including kinematic pitch-lag, pitch-flap, and elastic coupling. Hinge offset can also be represented. In addition, the hinge sequence can be changed from lag-flap to flap-lag by rotating θ_h from 0° to 90°. All of the blades are attached to a fixed hub which rotates at a constant speed, Ω.

Aerodynamic Theories

Before proceeding with the derivation of the equations of motion, the aerodynamic theories that are used will be briefly discussed. Since both the Theodorsen and Loewy theories are widely known, this discussion will serve only to compare their mathematical models and approaches. It will also point out the limitations their use imposes on the stability analysis.

The unsteady aerodynamic theory developed by Theodorsen [6] considers a thin airfoil undergoing simple harmonic motion, and being trailed by a straight wake. The vortex strength of this wake varies sinusoidally with time, and results in a lift deficiency function, C(k), which is associated only with the circulatory portion of the lift. This lift deficiency function is only dependent on the reduced frequency of the airfoil oscillations.

Loewy [7] modified the wake model in Theodorsen's analysis to more closely represent the case of a rotating wing. As shown in Figure 2, the airfoil section at any spanwise station is trailed by a wake in the plane of the rotor, as in Theodorsen's model. However, Loewy also includes vortex sheets below the plane of rotor, which result from the vorticity shed by previous passes of the blades being carried downward by the induced velocity. For ease of computation, the wake sheets are assumed to be parallel to the plane of rotation and without

to the plane of rotation and without curvature. They are also assumed to extend infinitely far ahead of and behind the airfoil, as well as below it.

Loewy's analysis of this aerodynamic model follows the same approach as that of Theodorsen, and the results are similar. The lift deficiency function $C(k,m,h,N,\psi_q)$, is again only associated with the circulatory lift. However, it is now dependent on the frequency ratio, the wake spacing, the number of blades, and the interblade phasing, as well as on the reduced frequency.

The quasi-steady approximation to the Theodorsen and Loewy theories is obtained by letting the lift deficiency function equal unity. This has no effect on the non-circulatory lift, but does make the circulatory lift independent of blade frequencies and wake geometry.

Since the lift deficiency functions of the unsteady theories are dependent on reduced frequency, a constraint is placed on the applicability of the stability analysis. That is, only those modes which have frequencies corresponding to the reduced frequency used to compute the value of the lift deficiency function are valid results. Therefore, unlike when the quasi-steady theory is used, a separate calculation must be made for each mode.

Another limitation on the validity of the stability analysis is applied when one is considering transient motion. Both Theodorsen's and Loewy's theories were developed only for simple harmonic airfoil motion. However, for lightly damped modes, the airfoil motion will be nearly simple harmonic.

$$e^{st} = e^{(\sigma+i\omega)t} = (e^{\sigma} e^{i\omega})^{t} \tag{1}$$

$$e^{\sigma} \cong 1 + \sigma + \sigma^2/2! + \ldots + \sigma^n/n! \tag{2}$$

Therefore, when the damping is small, e^{σ} is approximately unity and e^{st} is approximately $e^{i\omega t}$. This assumption of nearly simple harmonic motion essentially means that only the results for the lead-lag mode are valid, since

the damping of the flap mode is generally outside the limits of this approximation.

One final problem encountered when dealing with the Theodorsen and Loewy lift deficiency functions results from their being represented by complex numbers. If the resultant complex aerodynamic coefficients are not expressed in real form, the two eigenvalues for each mode will not necessarily be complex conjugates. The problems in physically interpreting such a solution are obvious. It is therefore necessary to invoke the assumption of simple harmonic or, in this case, nearly simple harmonic motion in order to express the aerodynamic coefficients as real numbers.

Equations of Motion

From Reference 5, the inertial and elastic moments about the hinges are

$$M_{\beta_i} = -\left\{\ddot{\beta} + 2\beta\dot{\zeta} + \left[1 + \frac{3}{2}\left(\frac{e}{1-e}\right)\right]\beta\right\} \tag{3}$$

$$M_{\zeta_i} = -\left[\ddot{\zeta} - 2\beta\dot{\beta} + \frac{3}{2}\left(\frac{e}{1-e}\right)\beta\right] \tag{4}$$

$$M_{\beta_e} = -\frac{1}{\Delta}\left\{\left[\bar{\omega}_\beta^2 + \left(\bar{\omega}_\zeta^2 - \bar{\omega}_\beta^2\right)\left(R_b \sin^2\theta_{b_o} + R_h \sin^2\theta_{h_o}\right)\right]\beta + \frac{1}{2}\left(\bar{\omega}_\zeta^2 - \bar{\omega}_\beta^2\right)\left(R_b \sin 2\theta_b + R_h \sin 2\theta_h\right)\zeta\right\} \tag{5}$$

$$M_{\zeta_e} = -\frac{1}{\Delta}\left\{\frac{1}{2}\left(\bar{\omega}_\zeta^2 - \bar{\omega}_\beta^2\right)\left(R_b \sin 2\theta_b + R_h \sin 2\theta_h\right)\beta + \left[\bar{\omega}_\zeta^2 - \left(\bar{\omega}_\zeta^2 - \bar{\omega}_\beta^2\right)\left(R_b \sin^2\theta_b + R_h \sin^2\theta_h\right)\right]\zeta\right\} \tag{6}$$

where

$$\Delta = 1 + \frac{\bar{\omega}_\zeta^2 - \bar{\omega}_\beta^2}{\bar{\omega}_\zeta^2\bar{\omega}_\beta^2}\left[R_b(1-R_b)\sin^2\theta_b + R_h(1-R_h)\sin^2\theta_h - R_bR_h\left(2\sin^2\theta_b \sin^2\theta_h + \frac{1}{2}\sin 2\theta_b \sin 2\theta_h\right)\right] \tag{7}$$

Since all of the aerodynamic theories used in this study are similar in form, the aerodynamic moments are derived for an arbitrary lift deficiency function, Q. The expressions for lift and drag are based on Reference 11, with the small pitch angle assumption removed.

$$L_{nc} = \frac{\rho a c}{2}\left(\frac{c}{4}\right)\left[\ddot{z}\cos\theta + \dot{z}\dot{\varepsilon}\sin\theta + \dot{V}\sin\theta + V\dot{\varepsilon}\cos\theta + \frac{c}{4}\ddot{\varepsilon}\right] \tag{8}$$

$$L_c = \frac{\rho a c}{2} V\left[\dot{z}\cos\theta + V\sin\theta + \frac{c}{2}\dot{\varepsilon}\right]Q \tag{9}$$

$$D = \frac{\rho a c}{2} V^2\left(\frac{C_{d_o}}{a}\right) \tag{10}$$

where

$$\dot{z} = -\left[\Omega\phi_i(e + x) + \dot{\beta}x\right]R \tag{11}$$

$$V = \left[\Omega(e + x) + \dot{\zeta}x\right]R \tag{12}$$

$$\dot{\varepsilon} = \Omega\sin\beta \tag{13}$$

Note that the blade vertical velocity, $\dot{z}$, contains contributions from the induced velocity and blade flapping; while V, the horizontal velocity, has contributions from the rotor rotation and the blade lead-lag motion. The terms containing $\dot{\varepsilon}$ are a result of the virtual pitch rate induced by the coning of the blade as it rotates.

To obtain the aerodynamic moments, Equations 11-13 are substituted into Equations 8-10, and the lift and drag resolved along the flap and lead-lag axes. The forces at each blade section are then multiplied by their moment arms about the hinge, and the product integrated over the span of the blade. The resulting moments are

$$M_{\beta_a} = \frac{\gamma}{8}\left\{(K_2e^2 + 2K_3e + K_4)(\sin\theta - \phi_i\cos\theta) - \left(\frac{\bar{c}}{4}K_3\cos\theta\right)\ddot{\beta}\right.$$
$$\left. + \left(\frac{\bar{c}}{8}K_3\sin 2\theta\right)\ddot{\zeta} - \left[(Q_2e - Q_3)\cos\theta\right]\dot{\beta}\right.$$

$$+ (Q_2 e + Q_3)(2 \sin\theta - \phi_i \cos\theta)\dot{\zeta} + \frac{\bar{c}}{4}\left[2(Q_1 e + Q_2) + (K_2 e + K_3)\cos^2\theta\right]\beta\Big\} \tag{14}$$

$$M_{\zeta_a} = -\frac{\gamma}{8}\Big\{(K_2 e^2 + 2K_3 e + K_4)\left[\phi_i(\sin\theta - \phi_i\cos\theta) + \frac{C_{d_o}}{a}\right] - \left(\frac{\bar{c}}{8} K_3 \sin 2\theta\right)\ddot{\beta} + \left(\frac{\bar{c}}{4} K_3 \sin^2\theta\right)\ddot{\zeta} + (Q_2 e + Q_3)(\sin\theta - 2\phi_i\cos\theta)\dot{\beta} + \left[(Q_2 e + Q_3)\phi_i \sin\theta + 2(K_2 e + K_3)\frac{C_{d_o}}{a}\right]\dot{\zeta} + \left[\frac{\bar{c}}{8}(K_2 e + K_3)\sin 2\theta\right]\beta\Big\} \tag{15}$$

where

$$K_n = \frac{4}{n}\left[(B-e)^n - x_o^n\right] \tag{16}$$

$$Q_n = 4\int_{x_o}^{B-e} x^n Q dx \tag{17}$$

The flap equation is obtained by summing Equations 3, 5, and 14, and setting the result equal to zero. Equations 4, 6, and 15 are summed and set equal to zero in order to obtain the lead-lag equation. By perturbing the blade about an equilibrium position, the equilibrium and perturbation equations are obtained.

$$\beta = \beta_o + \Delta\beta \tag{18}$$

$$\zeta = \zeta_o + \Delta\zeta \tag{19}$$

$$\theta = \theta_o + \theta_\beta \Delta\beta + \theta_\zeta \Delta\zeta \tag{20}$$

$$\theta_b = \theta_{b_o} + \theta_{\beta_b}\Delta\beta + \theta_{\zeta_b}\Delta\zeta \tag{21}$$

$$\theta_h = \theta_{h_o} + \theta_{\zeta_h} \Delta\beta + \theta_{\zeta_h} \Delta\zeta \tag{22}$$

The complete equations can be found in the appendix.

Multi-Bladed Rotor

When working with rotors having more than one blade, the standard practice is to transform the isolated blade equations into multi-blade coordinates [12]. Under this transformation, a four-bladed rotor would have four rotor degrees of freedom for each blade degree of freedom: collective, differential collective, lateral cyclic and longitudinal cyclic. In hover, the collective and differential collective degrees of freedom are linearly independent of each other and of the two cyclic degrees of freedom. The two cyclic degrees of freedom are, however, coupled.

Using quasi-steady or Theodorsen aerodynamics for the fixed hub, multi-bladed rotor considered in this investigation, the transformation to multi-blade coordinates provides little more information than would an isolated blade analysis. The results show the damping of all rotor modes to be the same for a single blade mode, and only the frequencies identify the high frequency ($\Omega + \omega$) and low frequency ($\Omega - \omega$) cyclic modes. This situation occurs because fixing the hub uncouples the blades from each other, and because the blades are aerodynamically independent. In addition, note that if the modal frequency, ω, is greater than the rotor speed, Ω; the low frequency cyclic mode is the progressing mode and the high frequency cyclic mode is the regressing mode. If $\omega < \Omega$, however, the low frequency mode becomes the regressing mode and the high frequency mode becomes the progressing mode.

The nature of the analysis changes when Loewy aerodynamics are introduced, since the blades are aerodynamically coupled through the wake structure. Each of the four independent rotor modes (collective, differential, low

frequency cyclic, and high frequency cyclic) resulting from the eigenanalysis have different wake geometries associated with them and, therefore, have different values of the interblade phasing, ψ_q.

$\psi_q = 0$	Collective
$\psi_q = \pi q$	Differential
$\psi_q = 2\pi q/N$	Low Frequency Cyclic
$\psi_q = \pi q(1 + 2/N)$	High Frequency Cyclic

Since the collective and differential degrees of freedom are independent in multi-blade coordinates, there are no difficulties in providing each set of equations with the proper aerodynamic coefficients. However, the fact that the cyclic degrees of freedom are coupled does present problems.

If the wake geometries associated with cyclic degrees of freedom are used to compute the aerodynamic coefficients for the coupled cyclic equations, the same damping is obtained for both the high and low frequency cyclic modes, irrespective of the differences in their wake geometries. The reason for this occurrence is that in both cyclic degrees of freedom the oscillations of each blade lead the one following it by $2\pi q/N$. Thus, the wake geometries of both cyclic degrees of freedom are the same, as are the aerodynamic coefficients. Since the hub is fixed, the damping must be the same for both modes.

There are two ways of circumventing these difficulties. The first is to consider only an isolated blade which is coupled to the others through the wake geometry [9]. This method is, however, only valid for a rotor with a fixed hub. The other way is to devise another transformation for the cyclic degrees of freedom which uncouples them and results in the proper wake geometries. For this case of the fixed hub, it is immaterial which method is

used. The flap-lag perturbation equations can be solved N times using the aerodynamic coefficients for a different mode each time; or be transformed into a set of 2N equations, each with the appropriate coefficients, and solved simultaneously.

Results and Discussion

A sampling of the results obtained from the above analysis are shown in Figures 3-7. In these figures, the configuration parameters are as given in Table 1, except where noted.

Figure 3 illustrates the effect of unsteady aerodynamics on a system with a low level of damping (note the scale of the ordinate). While the results using Theodorsen aerodynamics do differ from the quasi-steady results throughout the frequency range, the differences are small in comparison to the ones produced by using Loewy's aerodynamics. The addition of the wake sheets below the plane of the rotor appears to have a significant effect on the behavior of an isolated blade. There is a sharp spike at the 1/rev lead-lag frequency, an N-wave at 2/rev, and smaller dips at 3/rev and 4/rev.

The results for a four-bladed rotor (Fig. 4) show the same characteristics as those for the isolated blade. However, the peaks and valleys do not appear at every integer frequency for every mode. Instead, the collective mode has the 4/rev dip, the differential mode has the 2/rev N-wave, the low frequency cyclic mode has the 1/rev spike, and the high frequency cyclic mode has the 3/rev dip. Except at the points noted, these curves follow the Theodorsen curve quite closely. From other results, it appears that this pattern repeats itself at higher frequencies. That is, the collective mode would exhibit significant deviations from the Theodorsen curves at 4/rev, 8/rev, 12/rev, and so forth. The other modes would behave similarly. In addition, the sequence of low frequency cyclic at 1/rev, differential at 2/rev, high frequency cyclic

at 3/rev, and collective at 4/rev appears to hold for all other four-blade configurations.

With a system having a low level of damping, like the one above, a question arises as to whether the effect of Loewy aerodynamics is significant only for that type of system, or for all systems. To check out this possibility, a configuration with full elastic coupling and negative pitch-lag coupling was analyzed. The results (Fig. 5) show the wake effects to be significant only below lead-lag frequencies of 2.5/rev. It appears, therefore, that the wake effects become less significant as the level of damping in the system increases.

In order to determine if a torsionally soft blade would be more sensitive to Loewy aerodynamics than a torsionally rigid blade, a pseudo-torsional degree of freedom was added to the analysis. While the above analysis does not include the torsional degree of freedom, it can be approximated by using the pitch-flap and pitch-lag coupling parameters to produce pitch angle perturbations [11].

$$\theta_\beta = - \left[\left(\bar{\omega}_\zeta^2 - \bar{\omega}_\beta^2 \right) / \bar{\omega}_\theta^2 \, \bar{I}_\theta \right] \zeta_o \tag{23}$$

$$\theta_\zeta = - \left[\left(\bar{\omega}_\zeta^2 - \bar{\omega}_\beta^2 \right) / \bar{\omega}_\theta^2 \, \bar{I}_\theta \right] \beta_o \tag{24}$$

This approach neglects inertial torsion moments and is generally valid for torsion natural frequencies of 5.0 and above. Figure 6 shows the Loewy curve to have much larger deviations from the Theodorsen curve than in any other case. It should be noted, however, that the damping values in this case are of such a size as to make the assumption of simple harmonic motion somewhat questionable.

Finally, in order to see how the quasi-steady, Theodorsen and Loewy results compare for purely simple harmonic motion, a stability boundary was plotted for each (Fig. 7). For pitch angles below 0.1 radian and lead-lag

frequencies below 1/rev, all three are virtually identical. At higher pitch angles, the boundaries of the quasi-steady and unsteady theories diverge from one another. The main differences between the Loewy and Theodorsen results occur at and above 1/rev. At 1/rev, there is a small dip in the Loewy curve. Above that frequency, the curves intersect twice, indicating the type of behavior observed in the other figures.

Another significant feature of Figure 7 is the manner in which the Loewy effects do not diminish at the larger pitch angles. It is generally assumed that the effects of the wake sheets are more important at small pitch angles, where the wake sheets are more closely spaced. In the case of wake-induced bending-torsion flutter, decreases in wake spacing are destabilizing [9]. However, the pitch-flap problem is linear, and the aerodynamic coupling is independent of pitch angle. The flap-lag problem is, on the other hand, nonlinear and sensitive to aerodynamic coupling. As the flap-lag aerodynamic coupling increases with pitch angle, it overcomes the decrease in the wake effect caused by the increased spacing at higher pitch angles, and dominates the results.

Conclusions

The results of this investigation show that the choice of an aerodynamic theory can have a significant effect on stability calculations. Most notable is that the addition of wake sheets below the plane of the rotor influences the rotor stability characteristics. While this effect is not exceedingly large for most configurations, except at 1/rev, it does appear that it could be quite significant for systems having a low level of damping and for torsionally soft blades.

Secondly, it was shown that the method of multi-blade coordinates is not entirely applicable when Loewy aerodynamics are being used. It would also

appear that any aerodynamic theory with coefficients that depend on the wake geometry would not be compatible with multi-blade coordinates.

Finally, while the Loewy results are very interesting, the significant effects occur only at integer frequencies. Since rotor systems are designed to avoid these frequencies, the wake effects are observed where they have minimum influence. Consequently, for most practical configurations, they will probably not be quantitatively significant.

References

1. Hohenemser, K. H., and Heaton, P. W., "Aeroelastic Instability of Torsionally Rigid Helicopter Blades," Journal of the American Helicopter Society, Vol. 12, No. 2, April 1967.
2. Ormiston, R. A., and Hodges, D. H., "Linear Flap-Lag Dynamics of Hingeless Helicopter Rotor Blades in Hover," Journal of the American Helicopter Society, Vol. 17, No. 2, April 1972.
3. Friedmann, P., and Tong, P., "Non-linear Flap-Lag Dynamics of Hingeless Helicopter Blades in Hover and in Forward Flight," Journal of the Sound and Vibration, Vol. 3, No. 1, September 1973.
4. Ormiston, R. A., and Bousman, W. G., "A Theoretical and Experimental Investigation of Flap-Lag Stability of Hingeless Helicopter Rotor Blades," NASA TM X-62179, August 1972.
5. Bousman, W. G., Sharpe, D. L., and Ormiston, R. A., "An Experimental Study of Techniques for Increasing the Lead-Lag Damping of Soft Inplane Hingeless Rotors," Presented at the 32nd Annual AHS Forum, May 1976.
6. Theodorsen, T., "General Theory of Aerodynamic Instability and the Mechanism of Flutter," NACA Report 496, 1935.

7. Loewy, R. G., "A Two-Dimensional Approximation to the Unsteady Aerodynamics of Rotary Wings," Journal of the Aeronautical Sciences, Vol. 24, No. 2, February 1957.

8. Zvara, J., "The Aeroelastic Stability of Helicopter Rotors in Hovering Flight," MIT Aeroelastic and Structures Research Laboratory, ASRL TR 61-1, September 1956.

9. Anderson, W. D., and Watts, G. A., "Rotor Blade Wake Flutter," Lockheed-California Company, Lockheed Report LR 26213, December 1973.

10. Friedman, P., and Yuan, C., "Effect of Modified Aerodynamic Strip Theories on Rotor Blade Aeroelastic Stability," Proceedings of the 17th AIAA/ASME/SAE Structures, Structural Dynamics and Materials Conference, May 1976.

11. Hodges, D. H., and Ormiston, R. A., "Stability of Elastic Bending and Torsion of Uniform Cantilever Rotor Blades in Hover with Variable Structural Coupling," NASA TN D-8192, April 1976.

12. Hohenemser, K. H., and Yin, S. K., "Some Applications of the Method of Multi-Blade Coordinates," Journal of the American Helicopter Society, Vol. 17, No. 3, July 1973.

APPENDIX

Flap-Lag Equations with Unsteady Aerodynamics

Equilibrium Equations

$$\begin{bmatrix} \bar{F}_\beta & \bar{F}_\zeta \\ \bar{C}_\beta & \bar{C}_\zeta \end{bmatrix} \begin{Bmatrix} \beta_o \\ \zeta_o \end{Bmatrix} = \begin{Bmatrix} F_o \\ C_o \end{Bmatrix} \tag{A1}$$

$$\bar{F}_\beta = 1 + \frac{3}{2}\left(\frac{e}{1-e}\right) + \frac{1}{\Delta}\left[\bar{\omega}_\beta^{-2} + \left(\bar{\omega}_\zeta^{-2} - \bar{\omega}_\beta^{-2}\right)\left(R_b \sin^2 \theta_{b_o} + R_h \sin^2 \theta_{h_o}\right)\right] \tag{A2}$$

$$- \frac{\gamma \bar{c}}{32}(K_2 e + K_3)(2 + \cos^2 \theta_o)$$

$$\bar{F}_\zeta = \frac{\bar{\omega}_\zeta^{-2} - \bar{\omega}_\beta^{-2}}{2\Delta} \left(R_b \sin 2\theta_{b_o} + R_h \sin 2\theta_{h_o} \right) \tag{A3}$$

$$\bar{C}_\beta = \bar{F}_\zeta + \frac{\gamma \bar{c}}{64} (K_2 e + K_3) \sin 2\theta_o \tag{A4}$$

$$\bar{C}_\zeta = \frac{3}{2} \left(\frac{e}{1-} \right) + \frac{1}{\Delta} \left[\bar{\omega}_\zeta^{-2} - \left(\bar{\omega}_\zeta^{-2} - \bar{\omega}_\beta^{-2} \right) \left(R_b \sin^2 \theta_{b_o} + R_h \sin^2 \theta_{h_o} \right) \right] \tag{A5}$$

$$F_o = \frac{\gamma}{8} \left(K_2 e^2 + 2K_3 e + K_4 \right) (\sin \theta_o - \phi_i \cos \theta_o) \tag{A6}$$

$$C_o = - \frac{\gamma}{8} \left(K_2 e^2 + 2K_3 e + K_4 \right) \left[\phi_i (\sin \theta_o - \phi_i \cos \theta_o) + \frac{C_{d_o}}{a} \right] \tag{A7}$$

where

$$R_b = \left(\bar{\omega}_\zeta^{-2} K_\beta / K_{\beta b} \right) - \left(\bar{\omega}_\beta^{-2} K_\zeta / K_{\zeta b} \right) \Big/ \left(\bar{\omega}_\zeta^{-2} - \bar{\omega}_\beta^{-2} \right) \tag{A8}$$

$$R_h = \left(\bar{\omega}_\zeta^{-2} K_\beta / K_{\beta h} \right) - \left(\bar{\omega}_\beta^{-2} K_\zeta / K_{\zeta h} \right) \Big/ \left(\bar{\omega}_\zeta^{-2} - \bar{\omega}_\beta^{-2} \right) \tag{A9}$$

$$K_\beta = K_{\beta b} K_{\beta h} K_{\beta f} \Big/ \left(K_{\beta h} K_{\beta f} + K_{\beta b} K_{\beta f} + K_{\beta b} K_{\beta h} \right) \tag{A10}$$

$$K_\zeta = K_{\zeta b} K_{\zeta h} K_{\zeta f} \Big/ \left(K_{\zeta h} K_{\zeta f} + K_{\zeta b} K_{\zeta f} + K_{\zeta b} K_{\zeta h} \right) \tag{A11}$$

$$\bar{\omega}_\beta^{-2} = K_\beta / I\Omega^2 \tag{A12}$$

$$\bar{\omega}_\zeta^{-2} = K_\zeta / I\Omega^2 \tag{A13}$$

Perturbation Equations

$$\begin{bmatrix} F_{\ddot{\beta}} & F_{\ddot{\zeta}} \\ C_{\ddot{\beta}} & C_{\ddot{\zeta}} \end{bmatrix} \begin{Bmatrix} \ddot{\beta} \\ \ddot{\zeta} \end{Bmatrix} + \begin{bmatrix} F_{\dot{\beta}} & F_{\dot{\zeta}} \\ C_{\dot{\beta}} & C_{\dot{\zeta}} \end{bmatrix} \begin{Bmatrix} \dot{\beta} \\ \dot{\zeta} \end{Bmatrix} + \begin{bmatrix} F_\beta & F_\zeta \\ C_\beta & C_\zeta \end{bmatrix} \begin{Bmatrix} \beta \\ \zeta \end{Bmatrix} = \begin{Bmatrix} 0 \\ 0 \end{Bmatrix} \tag{A14}$$

$$F_{\ddot{\beta}} = 1 + \frac{\gamma \bar{c}}{32} K_3 \cos^2 \theta_o \tag{A15}$$

$$F_{\ddot{\zeta}} = - \frac{\gamma \bar{c}}{64} K_3 \sin 2\theta_o \tag{A16}$$

$$C_{\beta}^{\cdot\cdot} = F_{\zeta}^{\cdot\cdot} \tag{A17}$$

$$C_{\zeta}^{\cdot\cdot} = 1 + \frac{\gamma\bar{c}}{32} K_3 \sin^2 \theta_o \tag{A18}$$

$$F_{\beta}^{\bullet} = \frac{\gamma}{8} (Q_2 e + Q_3) \cos \theta_o \tag{A19}$$

$$F_{\zeta}^{\bullet} = 2\beta_o - \frac{\gamma}{8} (Q_2 e + Q_3)(2 \sin \theta_o - \phi_i \cos \theta_o) \tag{A20}$$

$$C_{\beta}^{\bullet} = -2\beta_o + \frac{\gamma}{8} (Q_2 e + Q_3)(\sin \theta_o - 2\phi_i \cos \theta_o) \tag{A21}$$

$$C_{\zeta}^{\bullet} = \frac{\gamma}{8} \left[(Q_2 e + Q_3)\theta_i \sin \theta_o + 2(K_3 e + K_4) \frac{C_{d_o}}{a} \right] \tag{A22}$$

$$F_{\beta} = 1 + \frac{3}{2} \left(\frac{e}{1-e}\right) + \frac{1}{\Delta} \left[\bar{\omega}_{\beta}^2 + \left(\bar{\omega}_{\zeta}^2 - \bar{\omega}_{\beta}^2 \right) \left(R_b \sin^2 \theta_{b_o} + R_h \sin^2 \theta_{h_o} \right) \right]$$

$$- \frac{\gamma\bar{c}}{32} \left[2(Q_1 e + Q_2) + (K_2 e + K_3) \cos^2 \theta_o \right] - F_1 \theta_{\beta} - F_2 \theta_{\beta_b} - F_3 \theta_{\beta_h} \tag{A23}$$

$$F_{\zeta} = \frac{\bar{\omega}_{\zeta}^2 - \bar{\omega}_{\beta}^2}{2\Delta} \left(R_b \sin 2\theta_{b_o} + R_h \sin 2\theta_{h_o} \right) - F_1 \theta_{\zeta} - F_2 \theta_{\zeta_b} - F_3 \theta_{\zeta_h} \tag{A24}$$

$$C_{\beta} = \frac{\bar{\omega}_{\zeta}^2 - \bar{\omega}_{\beta}^2}{2\Delta} \left(R_b \sin 2\theta_{b_o} + R_h \sin 2\theta_{h_o} \right) + \frac{\gamma\bar{c}}{64} (K_2 e + K_3 \sin 2\theta_o$$

$$- C_1 \theta_{\beta} - C_2 \theta_{\beta_b} - C_3 \theta_{\beta_h} \tag{A25}$$

$$C_{\zeta} = \frac{3}{2} \left(\frac{e}{1-e}\right) + \frac{1}{\Delta} \left[\bar{\omega}_{\zeta}^2 - \left(\bar{\omega}_{\zeta}^2 - \bar{\omega}_{\beta}^2 \right) \left(R_b \sin^2 \theta_{b_o} + R_h \sin^2 \theta_{h_o} \right) \right]$$

$$- C_1 \theta_{\zeta} - C_2 \theta_{\zeta_b} - C_3 \theta_{\zeta_h} \tag{A26}$$

where

$$F_1 = \frac{\gamma}{8} \left\{ \left(K_2 e^2 + 2K_3 e + K_4 \right)(\cos \theta_o + \phi_i \sin \theta) - \left[\frac{\bar{c}}{4} (K_2 e + K_3) \sin 2\theta_o \right] \beta_o \right\} \tag{A27}$$

$$F_2 = - \frac{R_b}{\Delta} \left(\bar{\omega}_{\zeta}^2 - \bar{\omega}_{\beta}^2 \right) \left[\left(\sin 2\theta_{b_o} - R_{wb} J_1 \right) \beta_o - \left(R_{wb} J_2 - \cos 2\theta_{b_o} \right) \zeta_o \right] \tag{A28}$$

$$F_3 = -\frac{R_h}{\Delta}\left(\bar{\omega}_\zeta^{-2} - \bar{\omega}_\beta^{-2}\right)\left[\left(\sin 2\theta_{h_o} - R_{wh}J_1\right)\beta_o - \left(R_{wh}J_2 - \cos 2\theta_{h_o}\right)\zeta_o\right] \quad \text{(A29)}$$

$$C_1 = -\frac{\gamma}{8}\left\{\left(K_2e^2 + 2K_3e + K_4\right)\phi_i(\cos\theta_o + \phi_i \sin\theta_o) + \left[\frac{\bar{c}}{4}\left(K_2e + K_3\right)\cos 2\theta_o\right]\beta_o\right\} \quad \text{(A30)}$$

$$C_2 = -\frac{R_b}{\Delta}\left(\bar{\omega}_\zeta^{-2} - \bar{\omega}_\beta^{-2}\right)\left[\left(\cos 2\theta_{b_o} - R_{wb}J_2\right)\beta_o - \left(\sin 2\theta_{b_o} + R_{wb}J_3\right)\zeta_o\right] \quad \text{(A31)}$$

$$C_3 = -\frac{R_h}{\Delta}\left(\bar{\omega}_\zeta^{-2} - \bar{\omega}_\beta^{-2}\right)\left[\left(\cos 2\theta_{h_o} - R_{wb}J_2\right)\beta_o - \left(\sin 2\theta_{h_o} + R_{wh}J_3\right)\zeta_o\right] \quad \text{(A32)}$$

and

$$J_1 = \frac{1}{\Delta}\left[\bar{\omega}_\beta^{-2} + \left(\bar{\omega}_\zeta^{-2} - \bar{\omega}_\beta^{-2}\right)\left(R_b \sin^2\theta_{b_o} + R_h \sin^2\theta_{h_o}\right)\right] \quad \text{(A33)}$$

$$J_2 = \frac{\bar{\omega}_\zeta^{-2} - \bar{\omega}_\beta^{-2}}{2\Delta}\left(R_b \sin 2\theta_{b_o} + R_h \sin 2\theta_{h_o}\right) \quad \text{(A34)}$$

$$J_3 = \frac{1}{\Delta}\left[\bar{\omega}_\zeta^{-2} - \left(\bar{\omega}_\zeta^{-2} - \bar{\omega}_\beta^{-2}\right)\left(R_b \sin^2\theta_{b_o} + R_h \sin^2\theta_{h_o}\right)\right] \quad \text{(A35)}$$

$$R_{wb} = \frac{\bar{\omega}_\zeta^{-2} - \bar{\omega}_\beta^{-2}}{\bar{\omega}_\zeta^{-2}\,\bar{\omega}_\beta^{-2}}\left[(1 - R_b)\sin 2\theta_{b_o} - R_h\left(2\sin^2\theta_{h_o}\sin 2\theta_{b_o} + \sin 2\theta_{h_o}\cos\theta_{b_o}\right)\right] \quad \text{(A36)}$$

$$R_{wh} = \frac{\bar{\omega}_\zeta^{-2} - \bar{\omega}_\beta^{-2}}{\bar{\omega}_\zeta^{-2}\,\bar{\omega}_\beta^{-2}}\left[(1 - R_h)\sin 2\theta_{h_o} - R_b\left(2\sin^2\theta_{b_o}\sin 2\theta_{h_o} + \sin 2\theta_{b_o}\cos\theta_{h_o}\right)\right] \quad \text{(A37)}$$

Table 1. Blade Configuration Parameters

$\gamma = 8$	Solidity = 0.05
$a = 2\pi$	$C_{d_o} = 0.01$
$R_h = 0$	
$\theta_{b_o} = 0$	$\theta_{h_o} = 0$
$\theta_\beta = \theta_{\beta_b} = 0$	$\theta_{\beta_h} = 0$
$\theta_\zeta = \theta_{\zeta_b}$	$\theta_{\zeta_h} = 0$
$e = 0$	$x_o = 0$
$B = 1.0$	

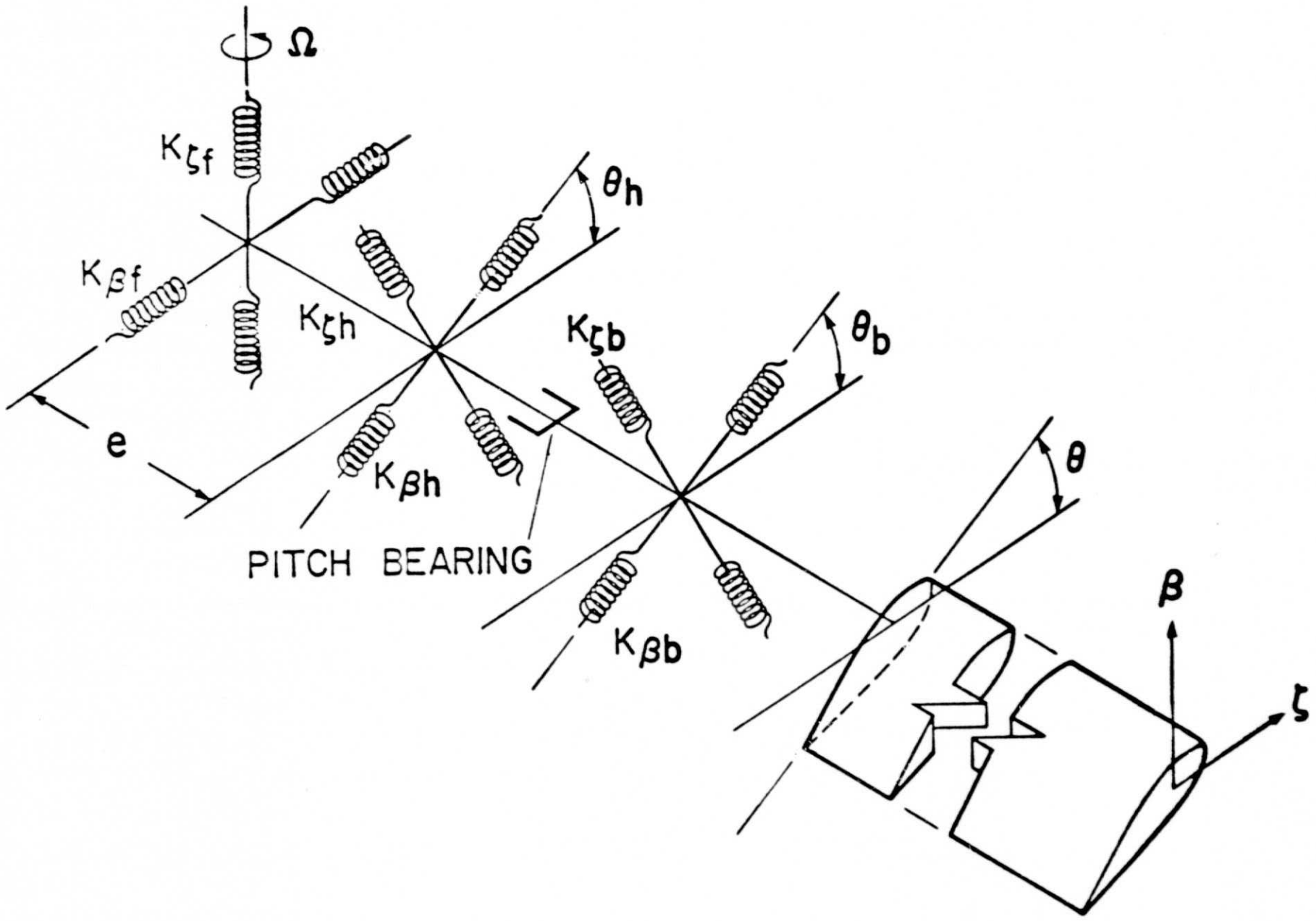

Figure 1. — Blade model.

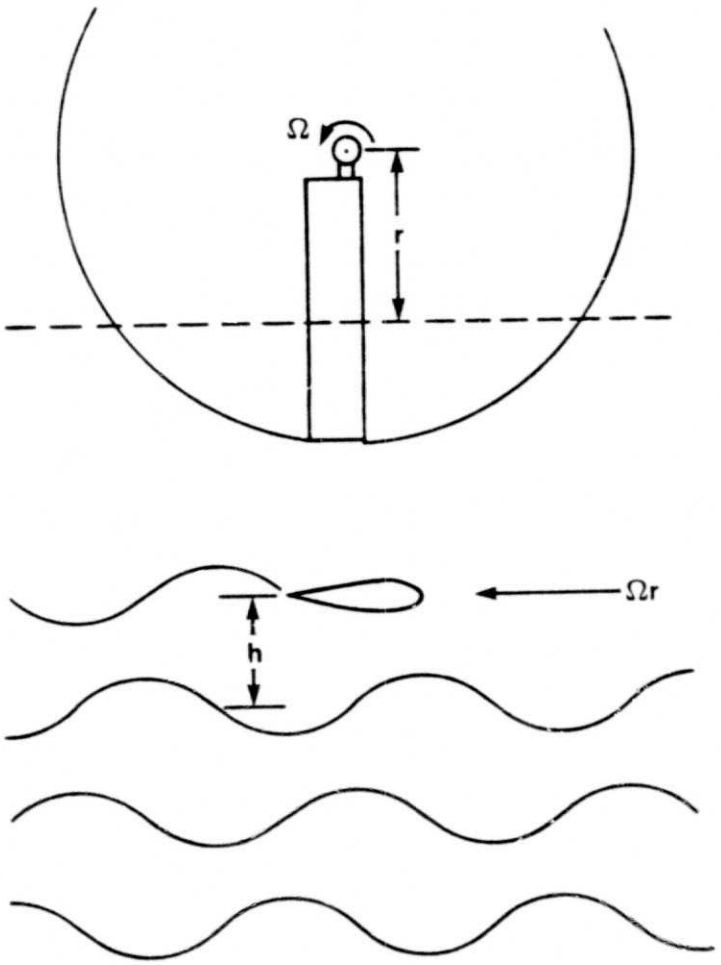

Figure 2. — Loewy's rotary wing model.

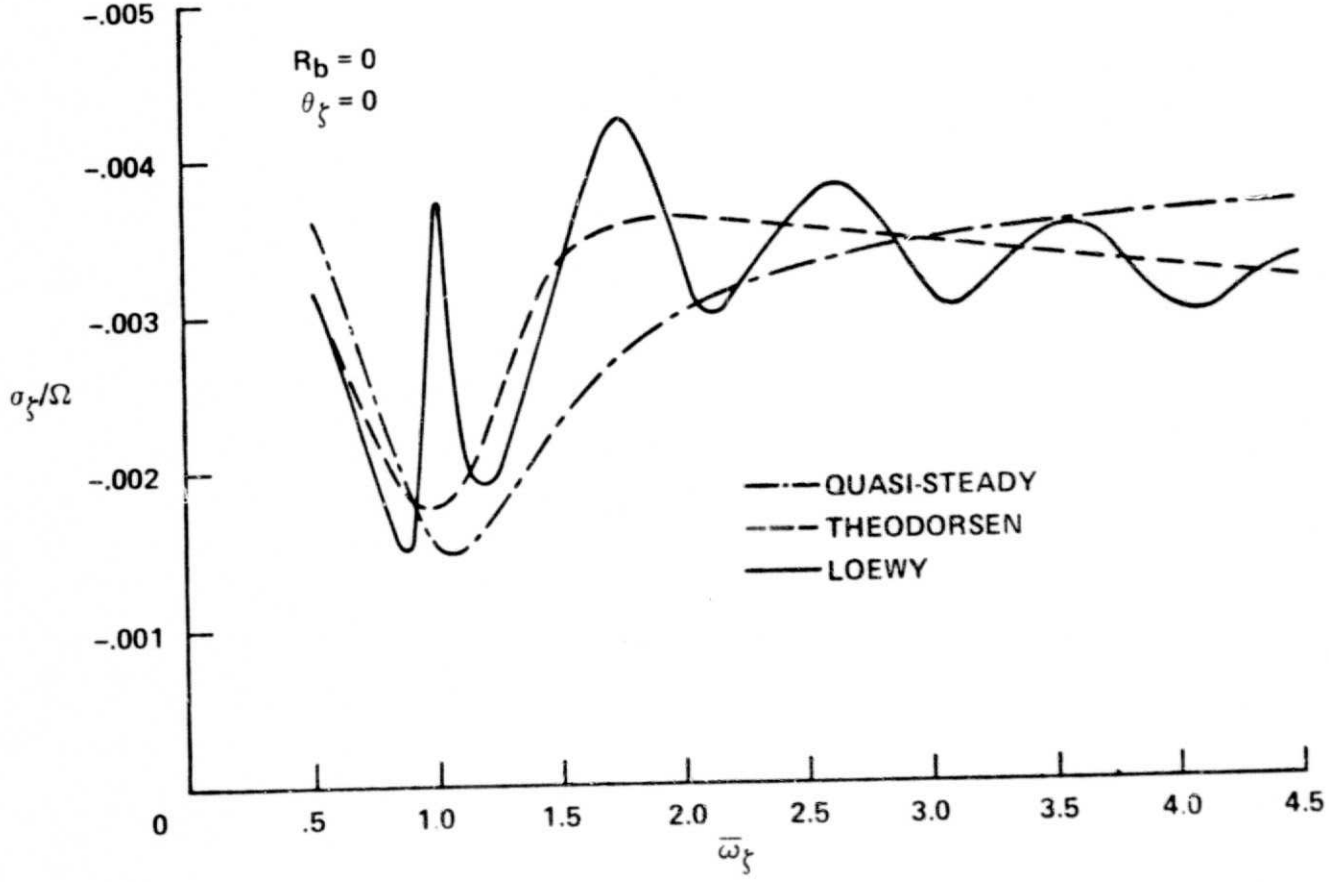

Figure 3. — Isolated blade (p = 1.10) at θ_o = 0.1 rad.

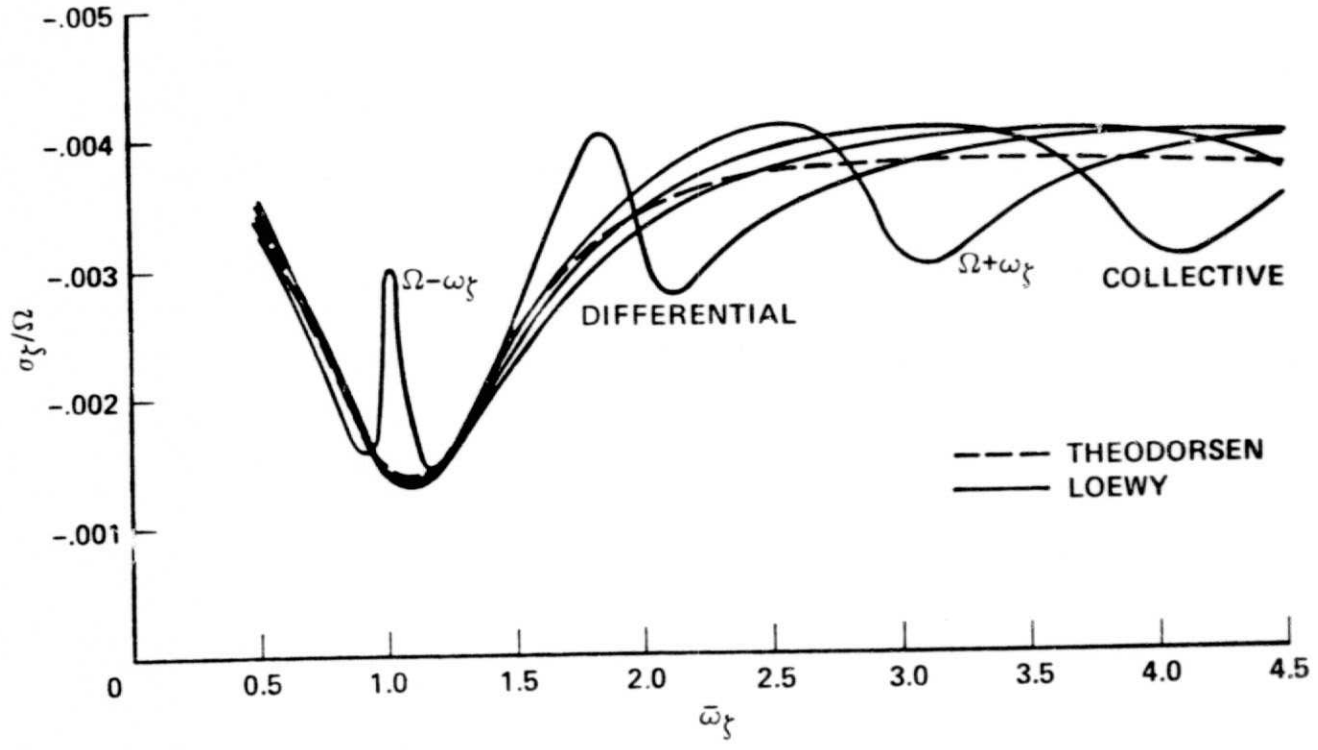

Figure 4. — Four-bladed rotor (p = 1.10) at θ_o = 0.1 rad.

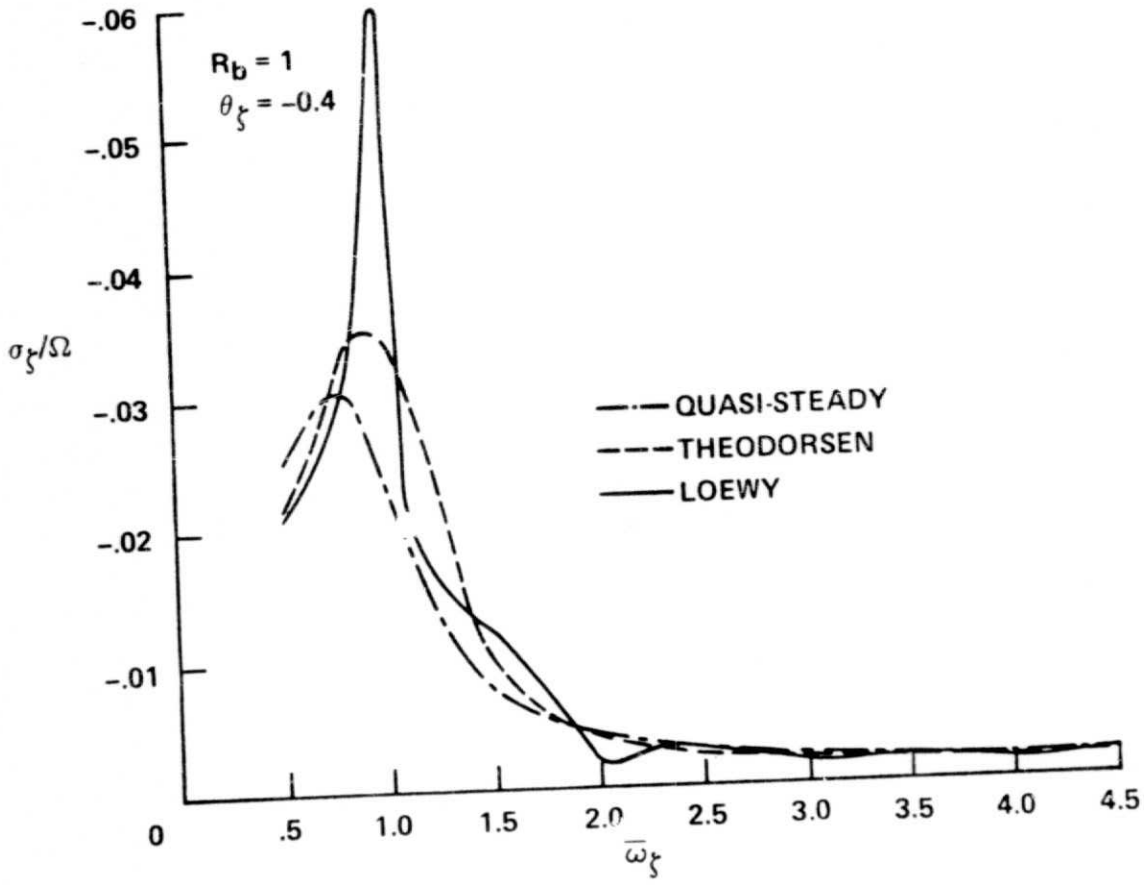

Figure 5. — Isolated blade (p = 1.10) at θ_o = 0.1 rad.

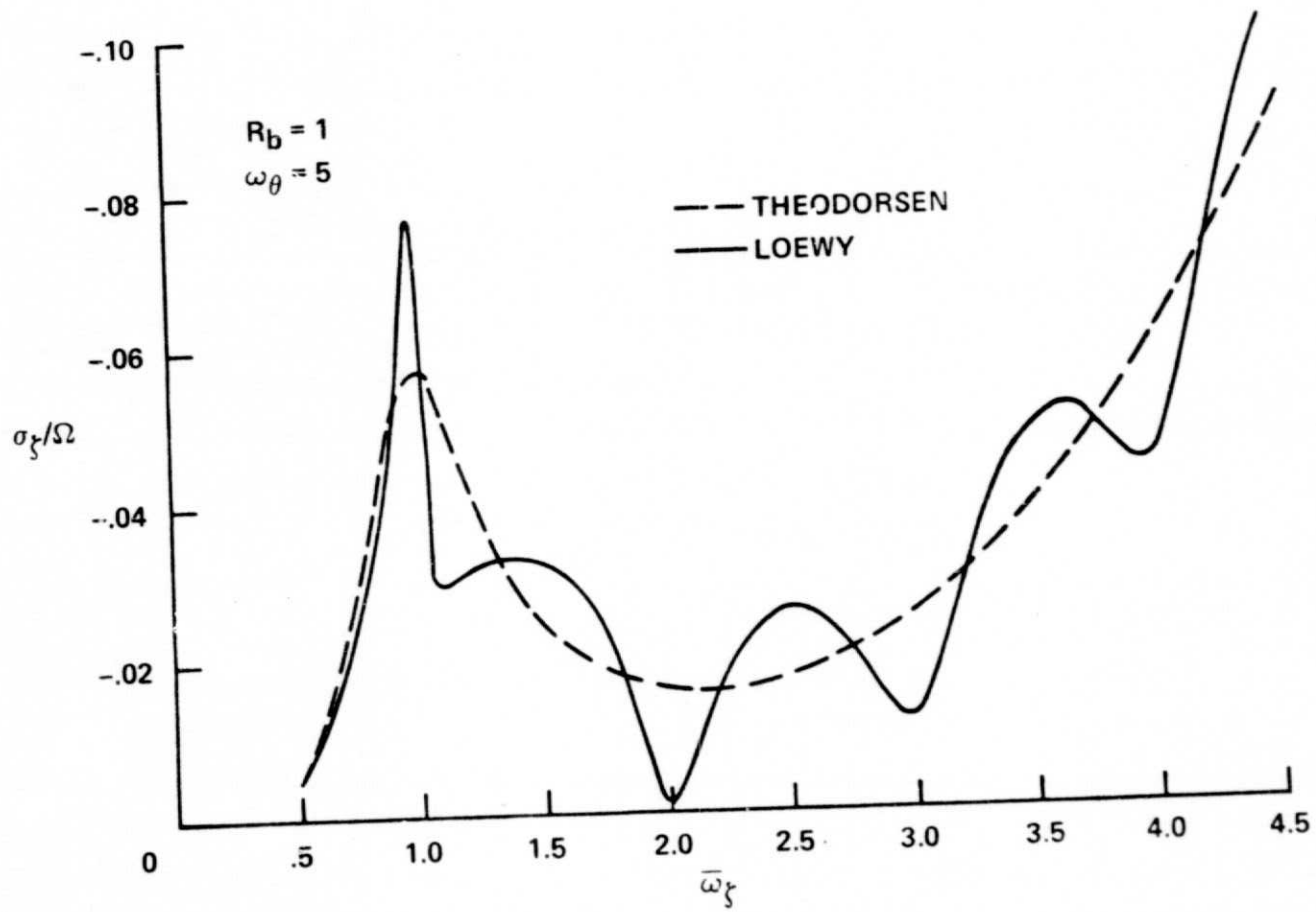

Figure 6. — Isolated blade (p = 1.10) with pseudo-torsional flexibility at θ_o = 0.1 rad.

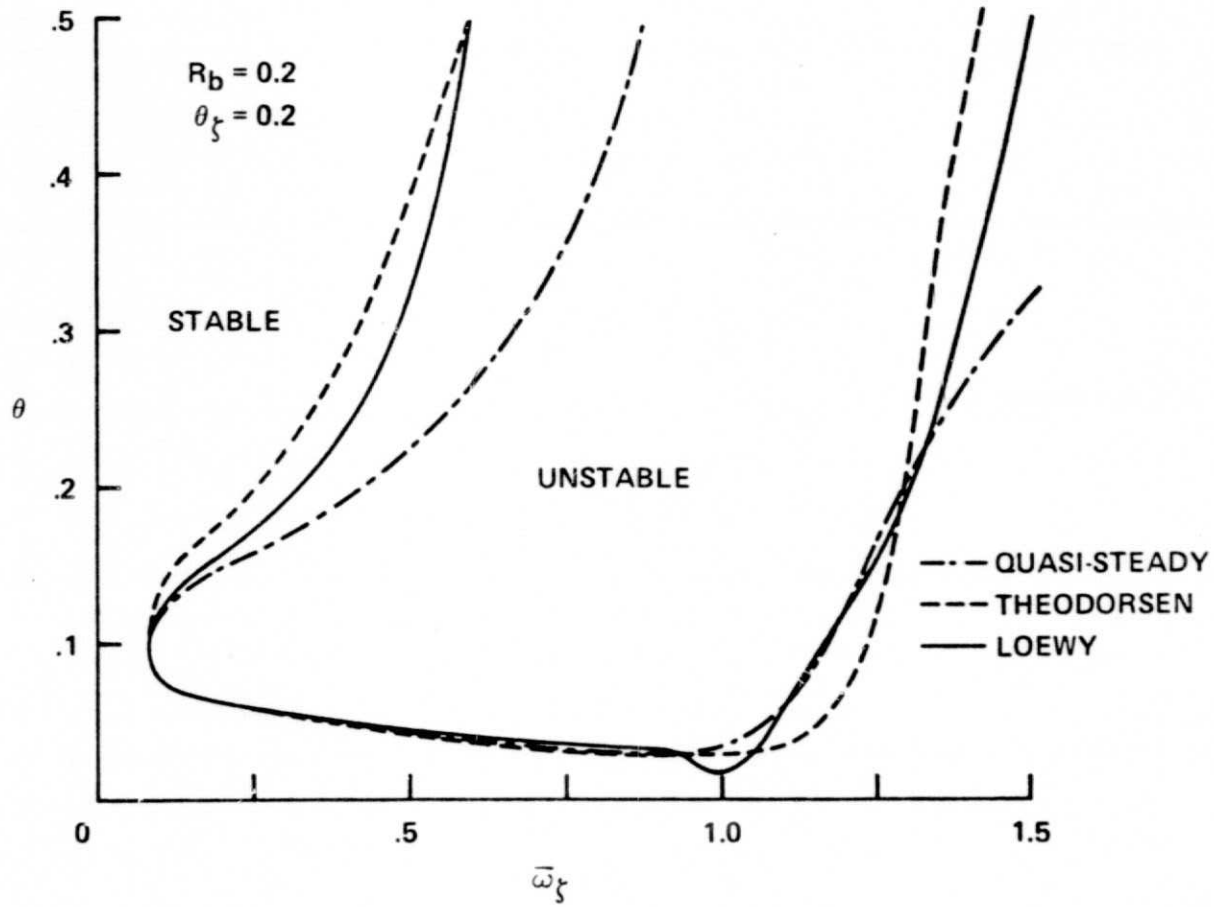

Figure 7. — Stability boundaries for an isolated blade with $p = \sqrt{4/3}$ and $\gamma = 5$.

1. Report No. NASA TM-78,434	2. Government Accession No.	3. Recipient's Catalog No.
4. Title and Subtitle EFFECTS OF UNSTEADY AERODYNAMICS ON ROTOR AEROELASTIC STABILITY		5. Report Date 6. Performing Organization Code
7. Author(s) Donald L. Kunz		8. Performing Organization Report No. A-7191 10. Work Unit No.
9. Performing Organization Name and Address Ames Research Center, NASA and Ames Directorate, USAAMRDL, AVRADCOM Ames Research Center, Moffett Field, Calif. 94035		11. Contract or Grant No. 13. Type of Report and Period Covered Technical Memorandum
12. Sponsoring Agency Name and Address National Aeronautics and Space Administration Washington, D.C. 20546		14. Sponsoring Agency Code
15. Supplementary Notes		

16. Abstract

An analysis was conducted to study the effects of unsteady aerodynamics on the stability characteristics of helicopter rotor blades. A simple physical model of each blade was used together with Theodorsen, Loewy, and quasi-steady aerodynamics to derive the equations of motion. The stability analysis comparing the effects of using each of the three theories revealed some significant differences between the Loewy and Theodorsen results. These included increases and decreases in lead-lag damping, localized around integer lead-lag frequencies. It was also shown that the standard method of multi-blade coordinates must be modified for use in conjunction with Loewy aerodynamics.

17. Key Words (Suggested by Author(s))	18. Distribution Statement		
Aeroelasticity Helicopter rotor Hingeless rotor Unsteady aerodynamics	Unlimited STAR Category - 02		
19. Security Classif. (of this report) Unclassified	20. Security Classif. (of this page) Unclassified	21. No. of Pages 29	22. Price* $3.75

*For sale by the National Technical Information Service, Springfield, Virginia 22161

1. Report No.	2. Government Accession No.	3. Recipient's Catalog No.
NASA TM-78,434		

4. Title and Subtitle	5. Report Date
EFFECTS OF UNSTEADY AERODYNAMICS ON ROTOR AEROELASTIC STABILITY	6. Performing Organization Code

7. Author(s)	8. Performing Organization Report No.
Donald L. Kunz	A-7191
	10. Work Unit No.

9. Performing Organization Name and Address	11. Contract or Grant No.
Ames Research Center, NASA and Ames Directorate, USAAMRDL, AVRADCOM Ames Research Center, Moffett Field, Calif. 94035	

12. Sponsoring Agency Name and Address	13. Type of Report and Period Covered
National Aeronautics and Space Administration Washington, D.C. 20546	Technical Memorandum
	14. Sponsoring Agency Code

15. Supplementary Notes

16. Abstract

An analysis was conducted to study the effects of unsteady aerodynamics on the stability characteristics of helicopter rotor blades. A simple physical model of each blade was used together with Theodorsen, Loewy, and quasi-steady aerodynamics to derive the equations of motion. The stability analysis comparing the effects of using each of the three theories revealed some significant differences between the Loewy and Theodorsen results. These included increases and decreases in lead-lag damping, localized around integer lead-lag frequencies. It was also shown that the standard method of multi-blade coordinates must be modified for use in conjunction with Loewy aerodynamics.

17. Key Words (Suggested by Author(s))	18. Distribution Statement
Aeroelasticity Helicopter rotor Hingeless rotor Unsteady aerodynamics	Unlimited STAR Category - 02

19. Security Classif. (of this report)	20. Security Classif. (of this page)	21. No. of Pages	22. Price*
Unclassified	Unclassified	29	$3.75

*For sale by the National Technical Information Service, Springfield, Virginia 22161